VBRI Press JOURNAL A RAPID PUBLICATION PLATFORM

Advanced Materials Letters

DOI: 10.5185/amlett.2015.()

Nanoindentation shows uniform local mechanical properties across melt pools and layers produced by selective laser melting of AlSi10Mg alloy

Nicola M. Everitt*, Nesma T. Aboulkhair, Ian Maskery, Chris J. Tuck, Ian Ashcroft

Department of Mechanical, Materials and Manufacturing Engineering, University of Nottingham, University Park, Nottingham NG2 7RD, United Kingdom

*Corresponding author: Tel (+44) 115 8466496; Email: nicola.everitt@nottingham.ac.uk

Received: --/--/2015, Revised: --/--/2015 and Accepted: --/--/2015

Abstract

Single track and single layer AlSi10Mg has been produced by selective laser melting (SLM) of alloy powder on a AlSi12 cast substrate. The SLM technique produced a cellular-dendritic ultra-fined grained microstructure. Chemical composition mapping and nanoindentation showed higher hardness in the SLM material compared to its cast counterpart. Importantly, although there was some increase of grain size at the edge of melt pools, nanoindentation showed that the hardness (i.e. yield strength) of the material was uniform across overlapping tracks. This is attributed to the very fine grain size and homogeneous distribution of Si throughout the SLM material.

Keywords (upto 5): nanoindentation, additive manufacturing, aluminium

1. INTRODUCTION

Additive manufacturing techniques have recently been gaining the attention of various industrial sectors to process a wide range of materials. Fabricating metal parts using an additive manufacturing approach can be done via a number of techniques such as direct metal laser sintering (DMLS), electron beam melting (EBM), and selective laser melting (SLM). These processes are appealing for the flexibility in manufacturing that they offer [1] besides enabling weight reduction through various routes, of which topology optimization and the use of lattice structures are examples [2]. During SLM, a part is built in a layer-by-layer fashion through metallurgical bonding between single scan tracks to form a layer and layers to form the 3D bulk sample. A schematic presentation of the process is shown in Figure 1. First a layer of powder with a pre-defined thickness is deposited on a heated build platform that is then scanned with a laser beam moving in the XY plane. After that, the piston controlled platform is lowered and the first step is repeated. These steps are successively repeated until the full part is built.

There are several studies in the literature investigating the processability of various alloys using SLM such as Ti alloys, stainless steels [3], Ni alloys [4] and Al alloys [5]. Al alloys are extensively used in the automotive and aerospace industries and being able to successfully process them using SLM is expected to further increase their feasibility in the industry. The literature has demonstrated the possibility of fabricating near fully dense parts from Al alloys using this technology [6,7] in addition to reporting outstanding mechanical performance when compared to the conventionally processed counterparts [8]. However, the studies available in the literature are mostly concerned with micro and macroscopic mechanical properties with little attention so far to the local mechanical properties, i.e. at the sub-micron level. From the authors' perspective, the local

mechanical properties could be rich with information for selectively laser melted materials, specifically Al alloys as their processing develops a characteristically fine microstructure [9].

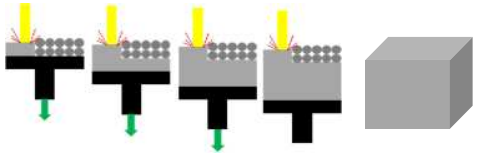

Figure 1 The principle of SLM

This work differs from other in the literature in that it used nanoindentation to explore the very local mechanical properties of the SLM material, and can link this nano-scale investigation to the detailed microstructure and chemical composition. Knowledge of the homogeneity (or not) of the mechanical properties of SLM material is necessary if the full potential of the technique is to be exploited in design of weight saving structures. The paper first establishes the hardness map across the melt pool produced below a single track, and then explores the differences produced by multiple tracks side by side in a single layer.

2. EXPERIMENTAL

2.1 Material Synthesis

The AlSi10Mg powder supplied by LPW technology, UK. A complete characterisation of the properties of the powder used in this study can be found in an earlier study published by the authors [10]. The AlSi10Mg is a specialty cast alloy widely used in the automotive industry. A cast slab of AlSi12 was used as a substrate onto which the scan tracks and layers were processed.

The single tracks and layers were produced using a Realizer SLM-50, Germany. The thickness of the powder layer laid down before a scan was made was 0.04 mm. The laser power was 100 W and production was carried out under an Ar atmosphere with oxygen content within the processing chamber below 0.1%. The scan speed was 250 mm s^{-1} and the spacing between the tracks to produce the layers was 0.05 mm. the hatch spacing 0.05 mm was used as it was shown to produce sufficient overlap between the scan tracks to yield a consolidated layer [6]. The single tracks and layers were cross-section and polished in preparation for the nanoindentation experiments.

2.2. Characterisation

Nanoindentation was carried out on a MicroMaterials Nanotest platform 3 (Micromaterials Ltd., Wrexham UK). A diamond Berkovoich indenter (3 sided pyramid) was used and the system calibrated using a fused silica reference sample. The test procedure carried out in accordance with ASTM E2546. Nanotest platform 3 (Micromaterials Ltd., Wrexham UK). A diamond Berkovoich indenter (3 sided pyramid) was used and the system calibrated using a fused silica reference sample. The test procedure carried out in accordance with ASTM E2546. In short, the load was increased at 0.375 mN S^{-1} up to a maximum load of 7.5mN and then unloaded at the same rate. A schematic is shown is Figure 2.

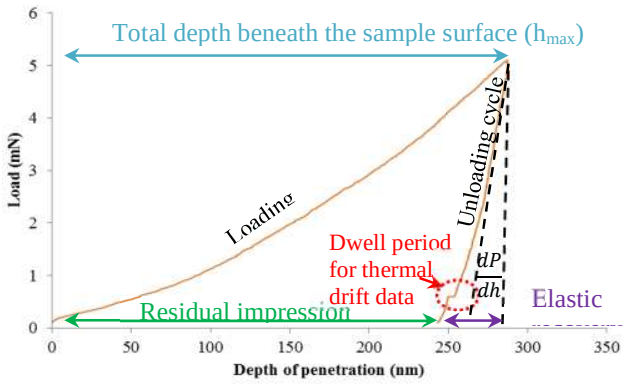

Figure 2 –Schematic of nanoindentation force/displacement data

In order to map the local properties across the melt pool(s) of the tracks or in the layers, indentations were spaced every 10 µm within a row and 15 µm between rows. Figure 3(a) shows an example of an array spanning across an individual melt pool and the cast substrate. In the work reported here, 308 indentations were used for the single track characterization, whilst 182 indentations were used in the layer array. A Hitachi TM2020 scanning electron microscope SEM equipped with an energy dispersive X-rays EDX detector served to determine the distribution of the chemical elements within the indented area.

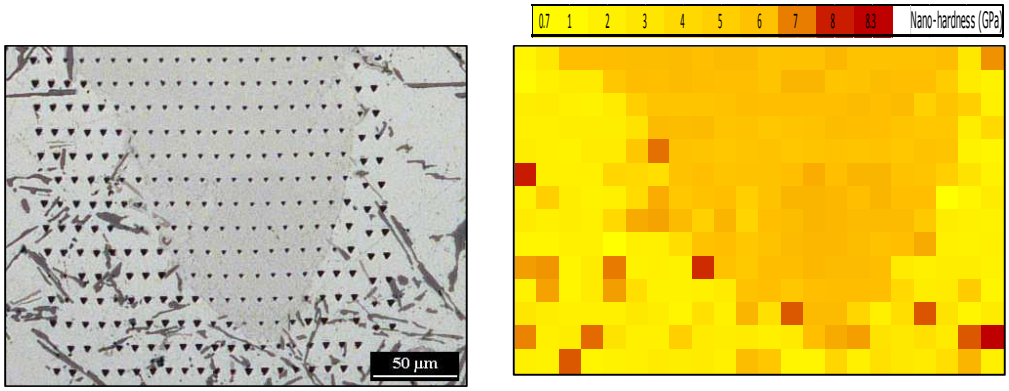

(a) (b)

Figure 3 (a) Array of indentations across the melt pool produced by a single track (b) Nanohardness map of that melt pool.

3. RESULTS & DISCUSSIONS

3.1 Single Track

The nanohardness of the melt pool of a single track was found to be 2. 21 GPa ± 0.01 (standard error). As illustrated by the hardness map in Fig 3(b) (and the small standard error of the hardness value), the hardness of the material in the melt pool is uniform with little spatial variation. This contrasts with the hardness of the as-cast structure of the AlSi12 alloy substrate with nanohardnesses varying from less than 1 GPa to more than 8 GPa. Specifically we have been able to link the high hardness to the Si flakes (shown in red in the chemical composition map in Figure 4) with a nanohardness of 9 ± 1 GPa, whilst the surrounding matrix in the as cast material microstructure has a nanohardness of 0.97 ± 1 GPa

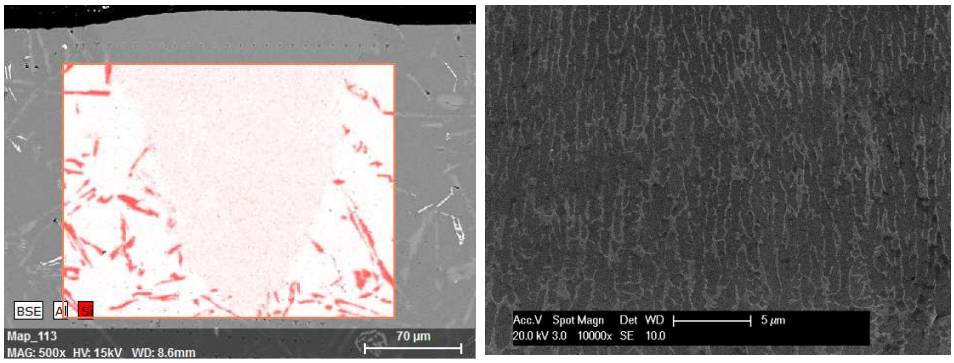

(a) (b)

Figure 4 (a) Chemical map of the melt pool beneath a single track and the surrounding substrate material. (Red = Si). (b) Microstructure of the melt pool material

The melt pool material shows a fine cellular-dendritic structure of α-Al surrounded by inter-dendritic Si (Fig 4(b)). This characteristic microstructure has been previously reported for selectively laser melted AlSi10Mg[11]. The high nanohardness and spatial uniformity of the hardness can be explained by the very fine grain size and uniform Si distribution which are all a function of the fast cooling rate inherent in the manufacturing process.

3.2 Layer

Having examined the microstructure of a single track, and also verified the power of nanoindentation to show up any spatial variation in nanohardness, we can now investigate any effect on the microstructure of each single track of the subsequent heating/cooling (remelting) produced by the next track. Figure 5 shows the hardness map across a layer composed of multiple tracks.

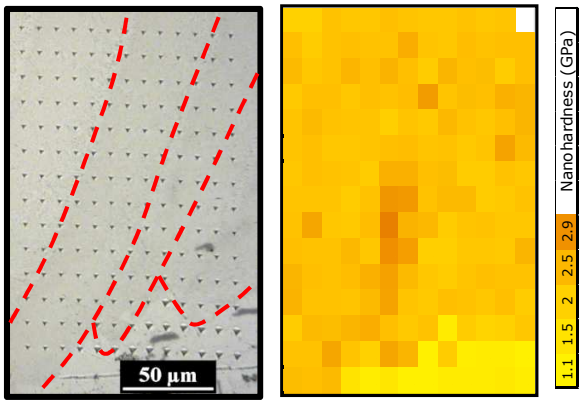

Figure 5 Single layer of SLM AlSi10Mg - Nanohardness map and the indentation array from which it is produced.(Red dotted lines show the location of the edge of the tracks).

The nanohardness of the single layer is remarkably uniform, with no signs of spatial variation at the edge of the tracks (melt pool boundaries). The average nanohardness of the single layer is 2.25 GPa (±0.02 standard error). The uniformity is perhaps surprising given the coarser microstructure which can be seen at the melt pool boundaries where the most secondary heating has taken place (Fig 6(a)). However the grain structure is still fine, and, more importantly, the Si is still homogenously distributed and has not redistributed to form the flakes seen in the as cast structure. For the investigated combination of processing parameters, the average nano-hardness within the single track with comparable to the single layer, supporting the observation that re-melting had no significant effect on altering the local mechanical properties.

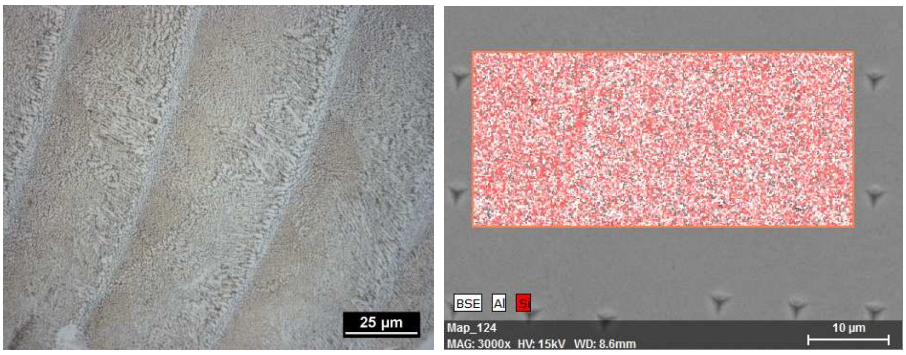

(a) (b)

Figure 6 (a) Etched microstructure of the SLM layer, (b) Chemical map of a representative area.

4. CONCLUSIONS

Selective laser melting of AlSi10Mg produced a cellular-dendritic ultra-fine-grained microstructure due to rapid solidification. Nanoindentation was able to distinguish the variation in microstructure of the as-cast substrate material. A higher mean nanohardness was recorded for the SLM melt pool and also across the surface of a whole layer which both showed uniform local mechanical properties. The uniform nano-hardness profile is attributed to the extremely fine microstructure along with the good dispersion of the alloying elements.

ACKNOWLEDGEMENTS

Funding is gratefully acknowledged from BBSRC (Everitt), EPSRC (Tuck and Ashcroft), and a Dean of Engineering Scholarship, UoN (Aboulkhair).

REFERENCES

1. Osakada, K.; Shiomi, M. *International Journal of Machine Tools and Manufacture* **2006**, *46*, 1188-93.
DOI: 10.1016/j.ijmachtools.2006.01.024
2. Maskery, I.; Aremu, A. O.; Simonelli, M.; Tuck, C. J.; Wildman, R. D.; Ashcroft, I.; Hague, R. J. M. *Experimental Mechanics* **2015**, *55*.
DOI: 10.1007/s11340-015-0021-5
3. Kamath, C.; El-dasher, B.; Gallegos, G.; King, W.; Sisto, A. *The International Journal of Advanced Manufacturing Technology* **2014**, *74*, 65-78.
DOI: 10.1007/s00170-014-5954-9
4. Carter, L. N.; Attallah, M. M.; Reed, R. C. at '*Proceedings of the International Symposium on Superalloys '* **2012**, 577-86.
5. Read, N.; Wang, W.; Essa, K.; Atallah, M. M. *Materials & Design* **2015**, *65*.
DOI: 10.1016/j.matdes.2014.09.044
6. Aboulkhair, N. T.; Everitt, N. M.; Ashcroft, I.; Tuck, C. J. *Additive Manufacturing* **2014**, *1*.
DOI: 10.1016/j.addma.2014.08.001
7. Buchbinder, D.; Schleifenbaum, H.; Heidrich, S.; Meiners, W.; Bültmann, J. *Physics Procedia* **2011**, *12, Part A*, 271-8.
DOI: 10.1016/j.phpro.2011.03.035
8. Kempen, K.; Thijs, L.; Van Humbeeck, J.; Kruth, J. P. *Physics Procedia* **2012**, *39*, 439-46.
DOI: 10.1016/j.phpro.2012.10.059
9. Thijs, L.; Kempen, K.; Kruth, J.-P.; Van Humbeeck, J. *Acta Materialia* **2013**, *61*, 1809-19.
DOI: 10.1016/j.actamat.2012.11.052
10. Aboulkhair, N. T.; Maskery, I.; Ashcroft, I.; Tuck, C. J.; Everitt, N. M. at '*22nd world congress of photonics: Lasers in Manufacturing'* **2015**.
11. Aboulkhair, N.; Tuck, C.; Ashcroft, I.; Maskery, I.; Everitt, N. *Metallurgical and Materials Transactions A* **2015**, *46*, 3337-41.
DOI: 10.1007/s11661-015-2980-7